An Inverter Fed With Combined Wind-Solar Energy System Using CUK-SEPIC Converter

Divya Teja Reddy Challa[1],   Raghavender Inguva[2]

(PG Scholar,Department of EEE, Teegala Krishna Reddy Engineering college, JNTU- Hyd, AP, INDIA)

** (Associate Professor,Department of EEE, Teegala Krishna Reddy engineering college, JNTU-Hyd, AP, INDIA)*

Abstract—Environmentally friendly solutions are becoming more prominent than ever as a result of concern regarding the state of our deteriorating planet. This paper presents an inverter fed with combination of two energy systems (wind, solar) using CUK-SEPIC converter. This configuration allows the two sources to supply the inverter separately or simultaneously depending on the availability of the energy sources. The inherent nature of this CUK-SEPIC fused converter, additional input filters are not necessary to filter out high frequency harmonics. Harmonic content is detrimental for the generator lifespan, heating issues, and efficiency. The fused multi-input rectifier stage also allows Maximum Power Point Tracking (MPPT) to be used to extract maximum power from the wind and sun when it is available. An adaptive MPPT algorithm will be used for the wind system and a standard perturb and observe method will be used for the PV system. Operational analysis of the proposed system will be discussed in this paper. Simulation results are given to highlight the merits of the proposed circuit

Keywords-MPPT -maximum power tracking, Inverter, CUK-SEPIC converter

I. INTRODUCTION

With increasing concern of global warming and the depletion of fossil fuel reserves, many are looking at sustainable energy solutions to preserve the earth for the future generations. Other than hydro power, wind and photovoltaic energy holds the most potential to meet our energy demands. Alone, wind energy is capable of supplying large amounts of power but its presence is highly unpredictable as it can be here one moment and gone in another. Similarly, solar energy is present throughout the day but the solar irradiation levels vary due to sun intensity and unpredictable shadows cast by clouds, birds, trees, etc. The common inherent drawback of wind and photovoltaic systems are their intermittent natures that make them unreliable. However, by combining these two intermittent sources and by incorporating maximum power point tracking (MPPT) algorithms, the system's power transfer efficiency and reliability can be improved significantly.

When a source is unavailable or insufficient in meeting the load demands, the other energy source can compensate for the difference. Several hybrid wind/PV power systems with MPPT control have been proposed and discussed in works [1] - [5]. Most of the systems in literature use a separate DC/DC boost converter connected in parallel in the rectifier stage as shown in Figure 1 to perform the MPPT control for each of the renewable energy power sources [1]-[4]. A simpler multi-input structure has been suggested by [5] that combine the sources from the DC-end while still achieving MPPT for each renewable source. The structure proposed by [5] is a fusion of the buck and buck-boost converter. The systems in literature require passive input filters to remove the high frequency current harmonics injected into wind turbine generators [6]. The harmonic content in the generator current decreases its lifespan and increases the power loss due to heating [6].

In this paper, an alternative multi-input rectifier structure is proposed for hybrid wind/solar energy systems. The proposed design is a fusion of the CUK and SEPIC converters. The features of the proposed topology are: 1) the inherent nature of these two converters eliminates the need for separate input filters for PFC [7]-[8]; 2) it can support step up/down operations for each renewable source (can support wide ranges of PV and wind input); 3) MPPT can be realized for each source; 4) individual and simultaneous operation is supported. The circuit operating principles will be discussed in this paper. Simulation results are provided to verify with the feasibility of the proposed system
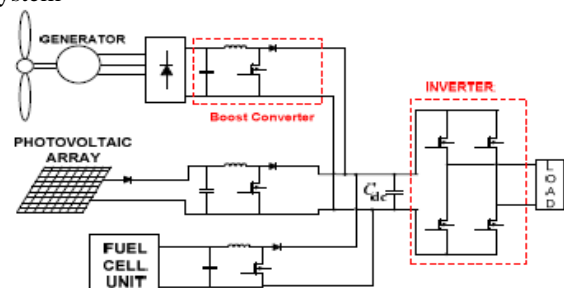

Figure 1: Hybrid system with multi-connected boost converter

II. PROPOSED MULTI-INPUT RECTIFIER STAGE

A system diagram of the proposed rectifier stage of a hybrid energy system is shown in Figure 2, where one of the inputs is connected to the output of the PV array and the other input connected to the output of a generator. The fusion of the two converters is achieved by reconfiguring the two existing diodes from each converter and the shared utilization of the CUK output inductor by the SEPIC converter. This configuration allows each converter to operate normally individually in the event that one source is unavailable. Figure 3 illustrates the case when only the wind source is available. In this case, D_1 turns off and D_2 turns on; the proposed circuit becomes a SEPIC converter and the input to output voltage relationship is given by (1). On the other hand, if only the PV source is available, then D_2 turns off and D_1 will always be on and the circuit becomes a CUK converter as shown in Figure 4. The input to output voltage relationship is given by (2). In both cases, both converters have step-up/down capability, which provide more design flexibility in the system if duty ratio control is utilized to perform MPPT control.

$$\frac{V_{dc}}{V_{W}} = \frac{d_2}{1-d_2} \qquad (1)$$

$$\frac{V_{dc}}{V_{PV}} = \frac{d_1}{1-d_1} \qquad (2)$$

Figure 5 illustrates the various switching states of the proposed converter. If the turn on duration of M_1 is longer than M_2, then the switching states will be state I, II, IV. Similarly, the switching states will be state I, III, IV if the switch conduction periods are vice versa. To provide a better explanation, the inductor current waveforms of each switching state are given as follows assuming that $d_2 > d_1$; hence only states I, III, IV are discussed in this example. In the following, $I_{i,PV}$ is the average input current from the PV source; $I_{i,W}$ is the RMS input current after the rectifier (wind case); and I_{dc} is the average system output current.

The key waveforms that illustrate the switching states in this example are shown in Figure 6. The mathematical expression that relates the total output voltage and the two input sources will be illustrated in the next section.

State I (M_1 on, M_2 on):

$$i_{L1} = I_{i,PV} + \frac{V_{PV}}{L_1}t \qquad 0 < t < d_1 T_s$$

$$i_{L2} = I_{dc} + \left(\frac{v_{c1} + v_{c2}}{L_2}\right)t \qquad 0 < t < d_1 T_s$$

$$i_{L3} = I_{i,W} + \frac{V_{W}}{L_3}t \qquad 0 < t < d_1 T_s$$

State III (M_1 off, M_2 on):

$$i_{L1} = I_{i,PV} + \left(\frac{V_{PV} - v_{c1}}{L_1}\right)t \qquad d_1 T_s < t < d_2 T_s$$

$$i_{L2} = I_{dc} + \frac{v_{c2}}{L_2}t \qquad d_1 T_s < t < d_2 T_s$$

$$i_{L3} = I_{i,W} + \frac{V_{W}}{L_3}t \qquad d_1 T_s < t < d_2 T_s$$

State IV (M_1 off, M_2 off):

$$i_{L1} = I_{i,PV} + \left(\frac{V_{PV} - v_{c1}}{L_1}\right)t \qquad d_2 T_s < t < T_s$$

$$i_{L2} = I_{dc} - \frac{V_{dc}}{L_2}t \qquad d_2 T_s < t < T_s$$

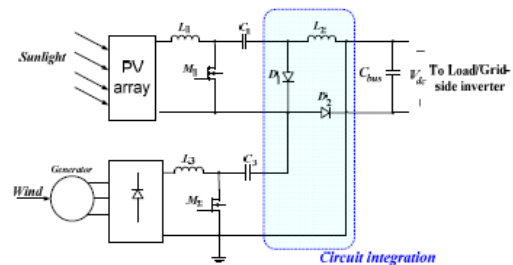$$i_{L3} = I_{i,W} + \left(\frac{V_{W} - v_{c2} - V_{dc}}{L_3}\right)t \qquad d_2 T_s < t < T_s$$

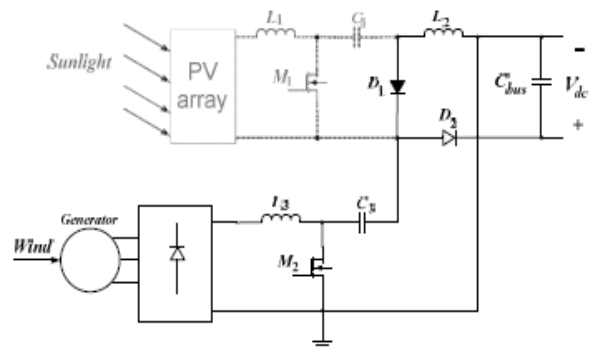Figure 2: Proposed rectifier stage for a Hybrid wind/PV system

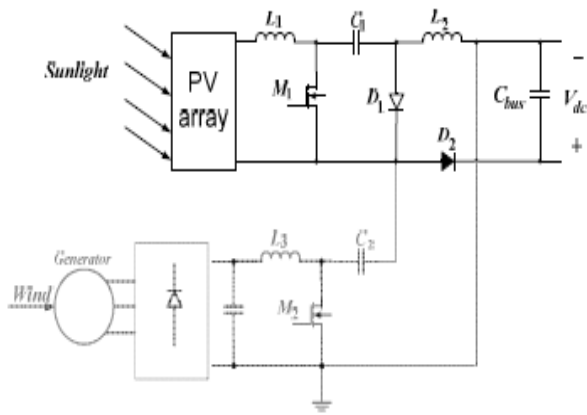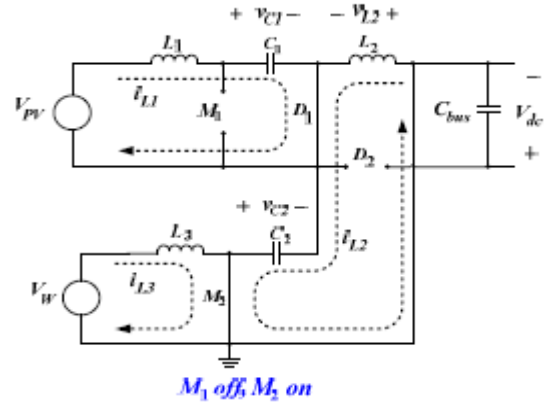
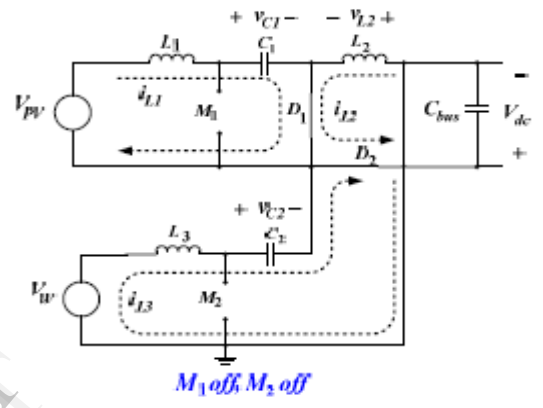Figure 3: Only wind source is operational (SEPIC)

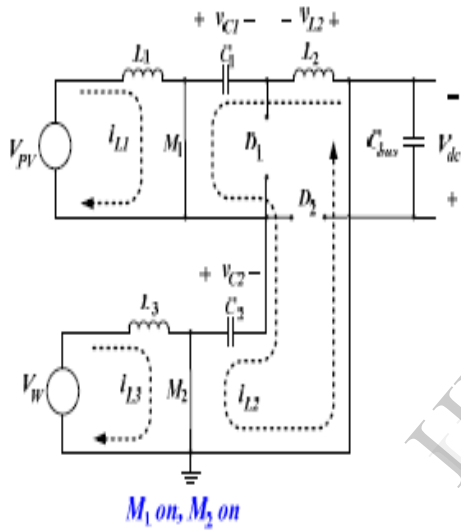Figure 4: Only PV source is operation (Cuk)
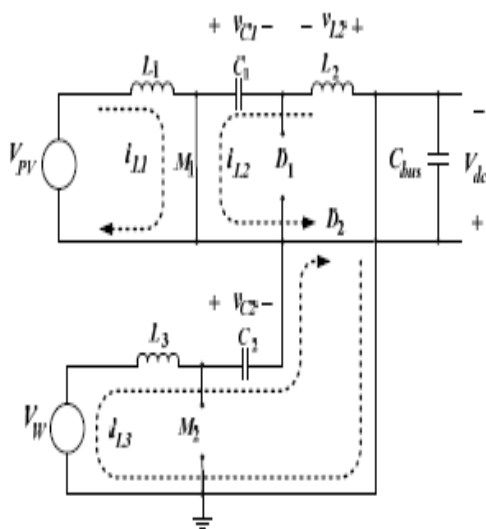
M₁ off, M₂ on

(III)

M₁ on, M₂ on

(I)

M₁ off, M₂ off

(IV)

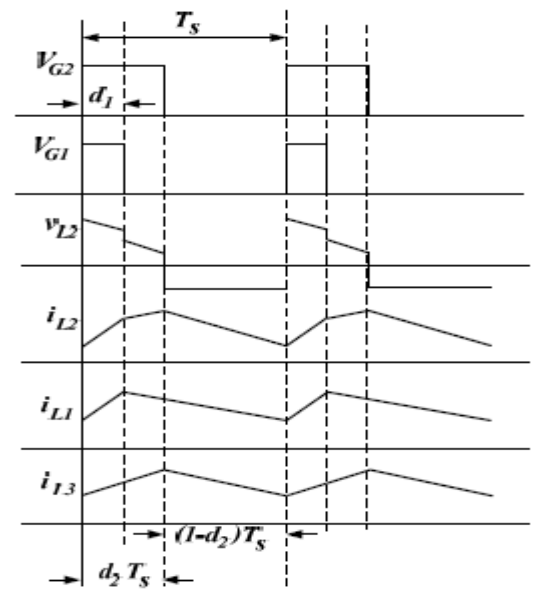Figure 5 (I-IV): switching states within a switching cycle

M₁ on, M₂ off

(II)

Figure 6: Proposed circuit inductor waveforms

III. ANALYSIS OF PROPOSED CIRCUIT

To find an expression for the output DC bus voltage, V_{dc}, the volt-balance of the output inductor, L_2, is examined according to Figure 6 with $d_2 > d_1$. Since the net change in the voltage of L_2 is zero, applying volt-balance to L_2 results in (3). The expression that relates the average output DC voltage (V_{dc}) to the capacitor voltages (v_{c1} and v_{c2}) is then obtained as shown in (4), where v_{c1} and v_{c2} can then be obtained by applying volt-balance to L_1 and L_3 [9]. The final expression that relates the average output voltage and the two input sources (V_W and V_{PV}) is then given by (5). It is observed that V_{dc} is simply the sum of the two output voltages of the CUK and SEPIC converter. This further implies that V_{dc} can be controlled by d_1 and d_2 individually or simultaneously.

$$(v_{c1} + v_{c2})d_1 T_s + (v_{c2})(d_2 - d_1)T_s + (1 - d_2)(-V_{dc})T_s = 0 \quad (3)$$

$$V_{dc} = \left(\frac{d_1}{1 - d_2}\right)v_{c1} + \left(\frac{d_2}{1 - d_2}\right)v_{c2} \quad (4)$$

$$V_{dc} = \left(\frac{d_1}{1 - d_1}\right)V_{PV} + \left(\frac{d_2}{1 - d_2}\right)V_w \quad (5)$$

The switches voltage and current characteristics are also provided in this section. The voltage stress is given by (6) and (7) respectively. As for the current stress, it is observed from Figure 6 that the peak current always occurs at the end of the on-time of the MOSFET. Both the Cuk and SEPIC MOSFET current consists of both the input current and the capacitors (C_1 or C_2) current. The peak current stress of M_1 and M_2 are given by (8) and (10) respectively. L_{eq1} and L_{eq2}, given by (9) and (11), represent the equivalent inductance of CUK and SEPIC converter respectively.

The PV output current, which is also equal to the average input current of the CUK converter, is given in (12). It can be observed that the average inductor current is a function of its respective duty cycle (d_1). Therefore by adjusting the respective duty cycles for each energy source, maximum power point tracking can be achieved.

$$v_{ds1} = V_{pv}\left(1 + \frac{d_1}{1 - d_1}\right) \quad (6)$$

$$v_{ds2} = V_w\left(1 + \frac{d_2}{1 - d_2}\right) \quad (7)$$

$$i_{ds1,pk} = I_{i,PV} + I_{dc,avg} + \frac{V_{PV} d_1 T_s}{2 L_{eq1}} \quad (8)$$

$$L_{eq1} = \frac{L_1 L_2}{L_1 + L_2} \quad (9)$$

$$i_{ds2,pk} = I_{i,W} + I_{dc,avg} + \frac{V_W d_2 T_s}{2 L_{eq2}} \quad (10)$$

$$L_{eq2} = \frac{L_3 L_2}{L_3 + L_2} \quad (11)$$

$$I_{i,PV} = \frac{P_o}{V_{dc}}\frac{d_1}{1 - d_1} \quad (12)$$

IV. MPPT CONTROL OF PROPOSED CIRCUIT

A common inherent drawback of wind and PV systems is the intermittent nature of their energy sources. Wind energy is capable of supplying large amounts of power but its presence is highly unpredictable as it can be here one moment and gone in another. Solar energy is present throughout the day, but the solar irradiation levels vary due to sun intensity and unpredictable shadows cast by clouds, birds, trees, etc. These drawbacks tend to make these renewable systems inefficient. However, by incorporating maximum power point tracking (MPPT) algorithms, the systems' power transfer efficiency can be improved significantly.

To describe a wind turbine's power characteristic, equation (13) describes the mechanical power that is generated by the wind [6].

$$p_m = 0.5 \rho A C_p(\lambda, \beta) v_w^3 \quad (13)$$

Where
$\rho = air\ density,$
$A = rotor\ swept\ area,$
$C_p(\lambda, \beta) = power\ coefficient\ function$
$\lambda = tip\ speed\ ratio,$
$\beta = pitch\ angle,$
$v_w = wind\ speed$

The power coefficient (C_p) is a nonlinear function that represents the efficiency of the wind turbine to convert wind energy into mechanical energy. It is dependent on two variables, the tip speed ratio (TSR) and the pitch angle. The TSR, λ, refers to a ratio of the turbine angular speed over the wind speed. The mathematical representation of the TSR is given by (14) [10]. The pitch angle, β, refers to the angle in which the turbine blades are aligned with respect to its longitudinal axis.

$$\lambda = \frac{R\ \omega_b}{v_w} \quad (14)$$

Where,
$\quad R = turbine\ radius$

ω_b = *angular rotational speed*

Figures 7 and 8 are illustrations of a power coefficient curve and power curve for a typical fixed pitch (β =0) horizontal axis wind turbine. It can be seen from figure 7 and 8 that the power curves for each wind speed has a shape similar to that of the power coefficient curve. Because the TSR is a ratio between the turbine rotational speed and the wind speed, it follows that each wind speed would have a different corresponding optimal rotational speed that gives the optimal TSR. For each turbine there is an optimal TSR value that corresponds to a maximum value of the power coefficient (C$_{p,max}$) and therefore the maximum power. Therefore by controlling rotational speed, (by means of adjusting the electrical loading of the turbine generator) maximum power can be obtained for different wind speeds.
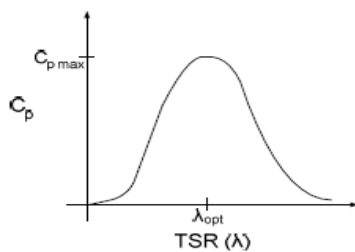

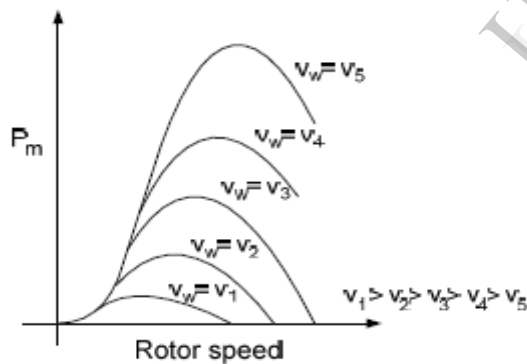Figure 7: Power Coefficient Curve for a typical wind turbine

Figure 8: Power Curves for a typical wind turbine

A solar cell is comprised of a P-N junction semiconductor that produces currents via the photovoltaic effect. PV arrays are constructed by placing numerous solar cells connected in series and in parallel [5]. A PV cell is a diode of a large-area forward bias with a photo voltage and the equivalent circuit is shown by Figure 9 [11]. The current-voltage characteristic of a solar cell is derived in [12] and [13] as follows:

$$I = I_{ph} - I_D \qquad (15)$$

$$I = I_{ph} - I_0\left[\exp\left(\frac{q(V + R_s I)}{Ak_B T}\right) - 1\right] - \frac{V + R_s I}{R_{sh}} \qquad (16)$$

Where
I_{ph} = *photocurrent,*
I_D = *diode current,*
I_0 = *saturation current,*
A = *ideality factor,*
q = *electronic charge 1.6x10-9,*
k_B = *Boltzmann's gas constant (1.38x10^{-23}),*
T = *cell temperature,*
R_s = *series resistance,*
R_{sh} = *shunt resistance,*
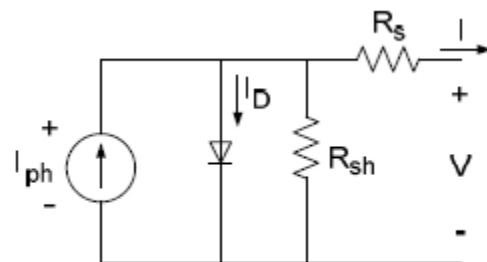I = *cell current,*
V = *cell voltage*

Figure 9: PV cell equivalent circuit

Typically, the shunt resistance (R$_{sh}$) is very large and the series resistance (R$_s$) is very small [5]. Therefore, it is common to neglect these resistances in order to simplify the solar cell model. The resultant ideal voltage-current characteristic of a photovoltaic cell is given by (17) and illustrated by Figure 10. [5]

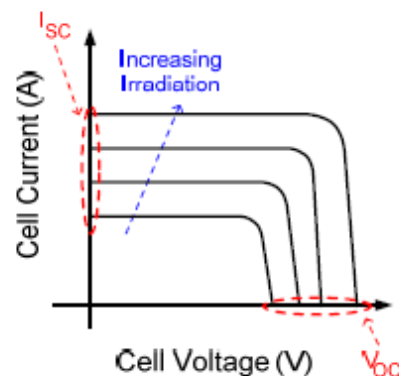$$I = I_{ph} - I_0\left(\exp\left(\frac{qV}{kT}\right) - 1\right) \qquad (17)$$

Figure 10: PV cell voltage-current characteristic

The typical output power characteristics of a PV array under various degrees of irradiation is illustrated by Figure 11. It can be observed in Figure 11 that there is a particular optimal voltage for each irradiation level that corresponds to maximum output power. Therefore by adjusting the output current (or

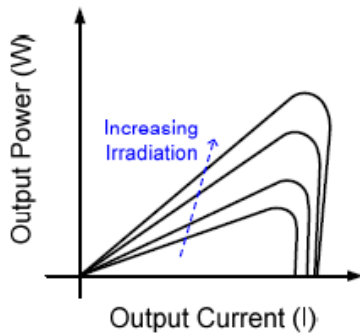voltage) of the PV array, maximum power from the array can be drawn.

Figure 11: PV cell power characteristics

Due to the similarities of the shape of the wind and PV array power curves, a similar maximum power point tracking scheme known as the hill climb search (HCS) strategy is often applied to these energy sources to extract maximum power. The HCS strategy perturbs the operating point of the system and observes the output. If the direction of the perturbation (e.g. an increase or decrease in the output voltage of a PV array) results in a positive change in the output power, then the control algorithm will continue in the direction of the previous perturbation. Conversely, if a negative change in the output power is observed, then the control algorithm will reverse the direction of the pervious perturbation step. In the case that the change in power is close to zero (within a specified range) then the algorithm will invoke no changes to the system operating point since it corresponds to the maximum power point (the peak of the power curves).

The MPPT scheme employed in this paper is a version of the HCS strategy. Figure 12 is the flow chart that illustrates the implemented MPPT scheme.

V. CONTROLLABLE PULSE WIDTH MODULATION

Pulse width modulation (PWM) is a powerful technique for controlling analog circuits with a microprocessor's digital outputs. PWM is employed in a wide variety of applications, ranging from measurement and communications to power control and conversion.

As power levels increase the task of designing variable drives increases dramatically. While the array of linear components available with sufficient voltage and current ratings for high power drives is impressive, a project can become unmanageable when calculation of internal power dissipation reveals the extent of cooling hardware required. Often the 20A drive requires multiple 20A semiconductors mounted on massive heat sinks, usually employs noisy fans and sometimes liquid cooling is mandated.

This slide illustrates the linear approach to delivering power to the load. When maximum output is commanded, the driver reduces resistance of the pass element to a minimum. At this output level, losses in the linear circuit are relatively low. When zero output is commanded the pass element approaches infinity and losses approach zero.

The disadvantage of the linear circuit appears at the midrange output levels and is often at its worst when 50% output is delivered. At this level, resistance of the pass element is equal to the load resistance which means heat generated in the amplifier is equal to the power delivered to the load! We have just found the linear circuit to have a maximum efficiency of 50% when driving resistive loads to mid-range power levels. When loads appear reactive, this efficiency drops even further.

VI. SIMULATION RESULTS

In this section, simulation results from MATLAB are given to verify that the proposed multi-input rectifier stage can support individual as well as simultaneous operation. The specifications for the design example are given in TABLE I. Figure 13 illustrates the system under the condition where the wind source has failed and only the PV source (CUK converter mode) is supplying power to the load. Figure 14 illustrates the system where only the wind turbine generates power to the load (SEPIC converter mode). Finally, Figure 17 illustrates the simultaneous operation (CUK-SEPIC fusion mode) of the two sources where M_2 has a longer conduction cycle.

TABLE I. Design Specifications

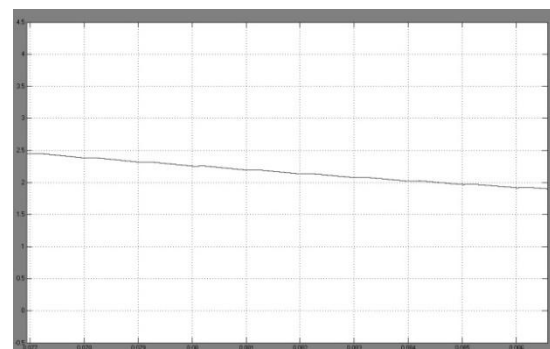|	
Output power (W)	3kW
Output voltage	500V
Switching frequency	20kHz

Fig.12 PV source output (CUK Operation)
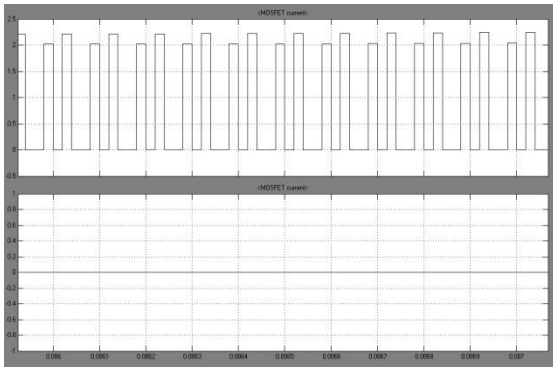
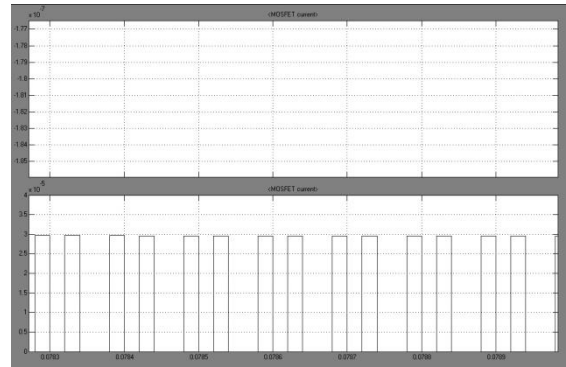Fig.13 Switches M1 and M2 currents when only solar is connected

When the CUK operation is performed wind source is going to off and the solar source is taking place and producing supply to the load at the output of a inverter is placed in the circuit .The output of the inverter is shown in the fig .15 and the output of the wind and solar is shown in fig 12,14. Here the wind output is AC and solar output is DC. SEPIC as well as CUK operation also performed which shown in fig.17.The switches M1 and M2 current waveforms are shown in figs.13 and 16 for CUK and SEPIC operations.
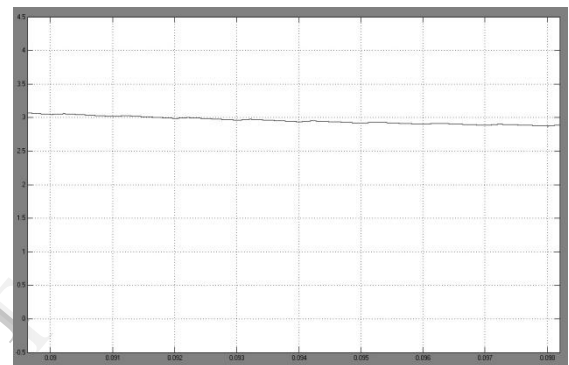

Fig.14 Wind Generator Output (SEPIC Operation)
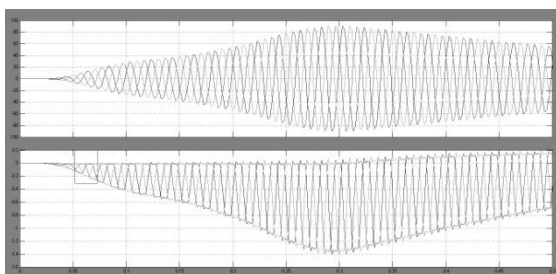
Fig.15 Output voltage and current of inverter

Fig.16 Switches M1 and M2 currents during CUK operation

Fig.17 Simultaneous operation with Wind and PV Source

VII. CONCLUSION

In this paper a new multi-input CUK-SEPIC rectifier stage for hybrid wind/solar energy systems has been presented. The features of this circuit are: 1) additional input filters are not necessary to filter out high frequency harmonics; 2) both renewable sources can be stepped up/down (supports wide ranges of PV and wind input); 3) MPPT can be realized for each source; 4) individual and simultaneous operation is supported. Simulation results have been presented to verify. Here the sinusoidal pulse width modulation technique is used for the inverter so that it will provide a better output results for the load.

REFERENCES

[1] S.K. Kim, J.H Jeon, C.H. Cho, J.B. Ahn, and S.H. Kwon, "Dynamic Modelling and Control of a Grid-Connected Hybrid Generation System with Versatile Power Transfer," IEEE Transactions on Industrial Electronics, vol. 55, pp. 1677-1688, April 2008.

[2] D. Das, R. Esmaili, L. Xu, D. Nichols, "An Optimal Design of a Grid Connected Hybrid

Wind/Photovoltaic/Fuel Cell System for Distributed Energy Production," in Proc. IEEE Industrial Electronics Conference, pp. 2499-2504, Nov. 2005.

[3] N. A. Ahmed, M. Miyatake, and A. K. Al-Othman, "Power fluctuations suppression of stand-alone hybrid generation combining solar photovoltaic/wind turbine and fuel cell systems," in Proc. Of Energy Conversion and Management, Vol. 49, pp. 2711-2719, October 2008.

[4] S. Jain, and V. Agarwal, "An Integrated Hybrid Power Supply for Distributed Generation Applications Fed by Nonconventional Energy Sources," IEEE Transactions on Energy Conversion, vol. 23, June 2008.

[5] Y.M. Chen, Y.C. Liu, S.C. Hung, and C.S. Cheng, "Multi-Input Inverter for Grid-Connected Hybrid PV/Wind Power System," IEEE Transactions on Power Electronics, vol. 22, May 2007.

[6] dos Reis, F.S., Tan, K. and Islam, S., "Using PFC for harmonic mitigation in wind turbine energy conversion systems" in Proc. of the IECON 2004 Conference, pp. 3100- 3105, Nov. 2004

[7] R. W. Erickson, "Some Topologies of High Quality Rectifiers" in the Proc. of the First International Conference on Energy, Power, and Motion Control, May 1997.

[8] D. S. L. Simonetti, J. Sebasti´an, and J. Uceda, "The Discontinuous Conduction Mode Sepic and ´ Cuk Power Factor Preregulators: Analysis and Design" IEEE Trans. On Industrial Electronics, vol. 44, no. 5, 1997

[9] N. Mohan, T. Undeland, and W Robbins, "Power Electronics: Converters, Applications, and Design," John Wiley & Sons, Inc., 2003.

[10] J. Marques, H. Pinheiro, H. Grundling, J. Pinheiro, and H. Hey, "A Survey on Variable-Speed Wind Turbine System," Proceedings of Brazilian Conference of Electronics of Power, vol. 1, pp. 732-738, 2003.

[11] F. Lassier and T. G. Ang, "Photovoltaic Engineering Handbook" 1990

[12] Global Wind Energy Council (GWEC), "Global wind 2008 report," June 2009.

[13] L. Pang, H. Wang, Y. Li, J. Wang, and Z. Wang, "Analysis of Photovoltaic Charging System Based on MPPT," Proceedings of Pacific-Asia Workshop on Computational Intelligence and Industrial Application 2008 (PACIIA '08), Dec 2008, pp. 498-50